

# Time-dependent CP violation in $B_s^0$ decays at LHCb

E. P. M. Gabriel

on behalf of the LHCb Collaboration

University of Edinburgh, Edinburgh EH8 9YL, United Kingdom

The  $B_s^0 - \bar{B}_s^0$  system can be used to look for new sources of CP violation. Time-dependent CP violation measurements of beauty mesons allow the determination of the mixing induced CP-violating phase,  $\phi_s$ . The angular analysis of the  $B_s^0 \rightarrow \phi\phi$  decay is presented, along with two  $B_s^0 \rightarrow J/\psi h^+ h^-$  decays, where the two hadrons are either a pair of kaons or a pair of pions. The analyses are based on data collected with the LHCb detector between 2011 and 2016.

## I. INTRODUCTION

The Standard Model (SM) fails to explain the matter-antimatter asymmetry observed in our universe. Finding new sources of CP violation could aid in explaining this difference. Time-dependent CP violation measurements of beauty mesons allow the determination of the mixing induced CP-violating phase,  $\phi_s$ . The CP-violating phase is of interest in both penguin dominated and three-level  $b \rightarrow s$  transitions, which test the flavour changing neutral current interaction describing B meson mixing. The LHCb experiment provides high sensitivity in these measurements.

We present new results of time-dependent CP violation in the  $B_s^0 - \bar{B}_s^0$  system using data collected at LHCb between 2011 and 2016. The analyses discussed are the time-dependent analysis of the  $B_s^0 \rightarrow \phi\phi$  decay, as well as two separate  $B_s^0 \rightarrow J/\psi h^+ h^-$  decays, where the two hadrons are either a pair of kaons or a pair of pions.

## II. MOTIVATION

In  $B_s^0$  decays that proceed through a  $b \rightarrow c\bar{c}s$  transition, the CP-violating phase,  $\phi_s^{c\bar{c}s}$  is given by  $-2\beta_s$  where higher order diagrams including loops and new physics (NP) contributions are neglected. This is analogous to the CKM-angle  $\beta$  in  $B^0$  decays. The CKM angle  $\beta_s$  is given by

$$\beta_s \equiv \arg \left( \frac{-V_{ts} V_{tb}^*}{V_{cs} V_{cb}^*} \right), \quad (1)$$

where the arguments are elements from the Cabibbo Kobayashi Maskawa (CKM) matrix.

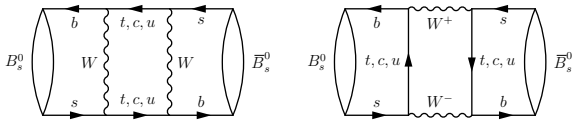


FIG. 1: The box diagrams representing  $B_s^0 - \bar{B}_s^0$  mixing.

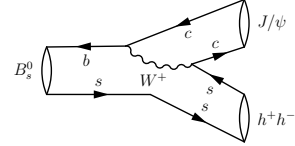


FIG. 2: The tree diagram of the  $B_s^0 \rightarrow J/\psi h^+ h^-$  decay.

The numerator arguments,  $V_{ts}$  and  $V_{tb}$ , stem from the  $B_s^0 - \bar{B}_s^0$  mixing Feynman diagram shown in Fig. 1. The two matrix elements in the denominator enter through the tree diagram of a  $b \rightarrow c\bar{c}s$  transition, as can be seen in Fig. 2. Thus, the CP-violating phase,  $\phi_s^{c\bar{c}s}$ , can be measured through interference between mixing and decay as  $\phi_s \equiv \phi_{\text{mix}} - 2\phi_{\text{dec}}$ .

## III. STATUS AND PREDICTIONS OF THE DECAYS

The updated measurement of CP violation parameters in the  $B_s^0 \rightarrow \phi\phi$  decay has been performed on the full Run 1 data-set with the addition of data collected in 2015 and 2016 [1]. The decay mode is dominated by penguin loop contributions, thus increasing the sensitivity to NP. In the analysis, the direct CP violation parameter,  $|\lambda|$  is measured, along with the CP-violating phase  $\phi_s^{s\bar{s}s}$ . The SM predicts  $\phi_s^{s\bar{s}s}$  close to zero in the context of QCD factorisation [2]. Theoretical errors are of the order of  $\sim 2\%$ [3]. However, several beyond the Standard Model (BSM) models allow for significant CP violation in  $b \rightarrow s\bar{s}s$  penguin decays [4–6].

The  $B_s^0 \rightarrow J/\psi h^+ h^-$  analyses are both performed using data collected by the LHCb detector in 2015 and 2016. The results have been combined with previous Run 1 measurements [7, 8]. The common parameters measured here are  $|\lambda|$  and the CP-violating phase  $\phi_s^{c\bar{c}s}$ .

The  $B_s^0 \rightarrow J/\psi K^+ K^-$  analysis [9] focuses on the  $\phi$  mass window by selecting the  $K^+ K^-$  invariant mass between  $0.99 \text{ GeV}/c^2$  and  $1.05 \text{ GeV}/c^2$ . Additional parameters measured in this decay are the decay width difference,  $\Delta\Gamma_s$ , as well as the difference between average decay widths,  $\Gamma_s - \Gamma_d$ .

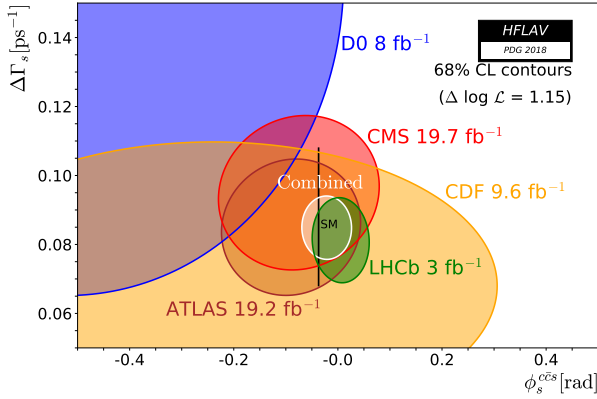


FIG. 3: Experimental status of  $\phi_s^{ccs}$  vs.  $\Delta\Gamma_s$  before the Winter 2019 conferences [10].

The  $B_s^0 \rightarrow J/\psi\pi^+\pi^-$  decay has previously been shown to have a predominant CP-odd final state [11]. This implies the decay has no sensitivity to  $\Gamma_L$ , such that the measured difference in average decay widths is  $\Gamma_H - \Gamma_d$ . Predictions from global fits to data of the phase  $\phi_s^{ccs}$  give a value of  $-36.8_{-1.0}^{+0.7}$  [mrad] [12]. Its experimental status before the Winter 2019 conferences is shown in Fig 3.

#### IV. ANALYSIS INGREDIENTS

The analyses discussed here are performed using a time-dependent angular analysis. The methods used are similar and a general overview of the necessary analysis ingredients is described in this section.

##### A. Selection

It is essential to select a sample of events with signal purity as high as possible. Each analysis uses different methods to achieve this. In the  $B_s^0 \rightarrow \phi\phi$  analysis, a multivariate neural network is trained to remove background events. The  $\Lambda_b^0 \rightarrow \phi p K^-$  background is modeled in the fit to the data due to it being difficult to remove. Roughly 8500 signal candidates were found in the full 2011-2016 data-set.

The  $B_s^0 \rightarrow J/\psi h^+ h^-$  analyses use a boosted decision tree to select signal events. In the  $B_s^0 \rightarrow J/\psi K^+ K^-$  decay mode, the  $\Lambda_b^0 \rightarrow J/\psi p K^-$  background mode is subtracted using negatively weighted MC candidates. A total of around 117 000 signal events are found. The  $B_s^0 \rightarrow J/\psi\pi^+\pi^-$  analysis uses the wrong sign ( $B_s^0 \rightarrow J/\psi\pi^\pm\pi^\pm$ ) invariant mass shape to determine the shape of the combinatorial background. This shape is used in the final mass fit, which yields roughly 33 500 signal candidates.

##### B. Decay-time resolution

To resolve the fast flavour oscillations induced by  $B_s^0 - \bar{B}_s^0$  meson mixing, it is essential to achieve a good decay-time resolution that is much smaller than the oscillation period. In the analyses covered here, an average decay-time resolution of 41 – 45 fs is accomplished.

The  $B_s^0 \rightarrow J/\psi h^+ h^-$  analyses make use of a prompt  $J/\psi$  sample to calibrate the decay-time resolution. In the  $B_s^0 \rightarrow \phi\phi$  analysis, a novel method was implemented, utilising the fact that the opening angle between the two kaons stemming from a  $\phi$  is very small. This is exploited by calibrating the decay-time resolution on a prompt pseudo-two body sample.

##### C. Angular efficiency

The non-uniform selection efficiency in the decay angles as a result of the LHCb detector acceptance and kinematic selection cuts needs to be accounted for. The helicity angles used in the  $B_s^0 \rightarrow J/\psi K^+ K^-$  decay are defined as shown in Fig. 4. A similar formalism is used in the  $B_s^0 \rightarrow \phi\phi$  and  $B_s^0 \rightarrow J/\psi\pi^+\pi^-$  analyses.

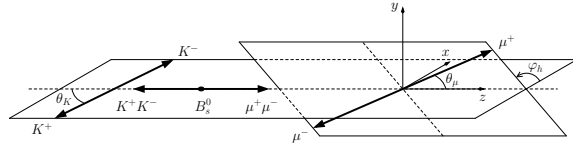


FIG. 4: Definition of the helicity angles used in the time-dependent angular  $B_s^0 \rightarrow J/\psi K^+ K^-$  analyses.

The efficiency is calculated for each analysis, where simulated events selected in the same way as data are used.

##### D. Decay-time efficiency

In a similar fashion, the decay-time efficiency needs to be accounted for. All Run 2 (2015-2016) data uses the  $B^0 \rightarrow J/\psi K^{*0}$  decays as a control mode. A different control sample is used in Run 1 vs. Run 2 data due to differences in the higher level trigger configuration. In order to create a control sample that is kinematically more similar to the decay mode of interest, the Run 1  $B_s^0 \rightarrow \phi\phi$  data use the control mode  $B_s^0 \rightarrow D_s^- \pi^+$ .

### E. Flavour tagging

Knowledge of the flavour of the  $B_s^0$  meson at production is essential in measuring the CP-violating phase  $\phi_s$ , since the sensitivity to the phase scales directly with the effective tagging power. At LHCb, flavour tagging algorithms are generated using self-tagged decay modes, such as  $B^+ \rightarrow J/\psi K^+$  and  $B_s^0 \rightarrow D_s^- \pi^+$ . The effective tagging power achieved in the analyses discussed here is roughly 5%.

## V. RESULTS

The time-dependent fit to extract the CP violation parameters consists of a simultaneous fit to the decay-time and the three helicity angles. The  $B_s^0 \rightarrow \phi\phi$  fit consists of three contributions: the CP-even  $P$ -wave and CP-odd  $P$ -wave coming from the  $\phi\phi$  final state. In addition, the  $f_0(980)$  resonance is close in mass to the  $\phi$  and could thus contribute to the result. This is accounted for in the fit by allowing the combination of an  $S$ -wave and double  $S$ -wave component. The fit results are given in Tab. I. The results presented are in agreement with previous LHCb results as well as the SM predictions.

 TABLE I:  $B_s^0 \rightarrow \phi\phi$  results

Parameter	Fit Result
$\phi_s^{s\bar{s}s}$	$-0.073 \pm 0.115 \pm 0.027$ [rad]
$ \lambda $	$0.99 \pm 0.05 \pm 0.01$

To extract the fit parameters in the  $B_s^0 \rightarrow J/\psi K^+ K^-$  analysis a similar procedure is used. The difference is that the  $m(K^+ K^-)$  invariant mass is split into six bins. This aids in controlling the interference of the  $\phi$  component with the  $S$ -wave  $f_0(980)$  contribution. The time-dependent angular fit consists of a simultaneous fit in decay-time and helicity angles in the six two-kaon mass bins. The results are shown in Tab. II. These are the most precise single measurements of  $\phi_s^{c\bar{c}s}$ ,  $\Gamma_s - \Gamma_d$  and  $\Delta\Gamma_s$ . The results are in agreement with SM predictions.

 TABLE II:  $B_s^0 \rightarrow J/\psi K^+ K^-$  results

Parameter	Fit Result
$\phi_s^{c\bar{c}s}$	$-0.083 \pm 0.041 \pm 0.006$ [rad]
$ \lambda $	$1.012 \pm 0.016 \pm 0.006$
$\Gamma_s - \Gamma_d$	$-0.0041 \pm 0.0024 \pm 0.0015$ [ps $^{-1}$ ]
$\Delta\Gamma_s$	$-0.0772 \pm 0.0077 \pm 0.0026$ [ps $^{-1}$ ]

The  $B_s^0 \rightarrow J/\psi\pi^+\pi^-$  analysis performs a simultaneous fit to the decay-time, helicity angles and the

$\pi^+\pi^-$  mass spectrum. The fit to the  $\pi^+\pi^-$  invariant mass, displayed in Fig. 5, consists of many resonances. The biggest contribution comes from the  $f_0(980) \rightarrow \pi^+\pi^-$ . Other components in the fit are the  $f_0(1790)$ ,  $f_2(1270)$ ,  $f_2'(1525)$  and non-resonant contributions. The results are shown in Tab. III.

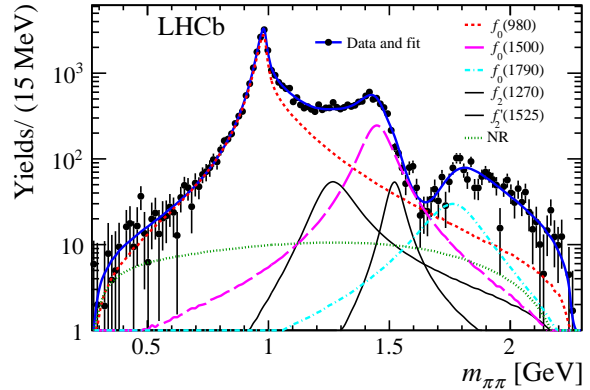

 FIG. 5: A fit to the  $\pi^+\pi^-$  invariant mass in the  $B_s^0 \rightarrow J/\psi\pi^+\pi^-$  analysis.

 TABLE III:  $B_s^0 \rightarrow J/\psi\pi^+\pi^-$  results

Parameter	Fit Result
$\phi_s^{c\bar{c}s}$	$-0.057 \pm 0.060 \pm 0.011$ [rad]
$ \lambda $	$1.01^{+0.08}_{-0.06} \pm 0.03$
$\Gamma_H - \Gamma_d$	$-0.050 \pm 0.004 \pm 0.004$ [ps $^{-1}$ ]

## VI. $\phi_s^{c\bar{c}s}$ COMBINATION

The LHCb collaboration has performed many measurements of the CP-violating phase,  $\phi_s^{c\bar{c}s}$ , in  $b \rightarrow c\bar{c}s$  transitions. The LHCb combined result shown in Fig. 3 includes results using Run 1 data taken at the LHCb detector from  $B_s^0 \rightarrow \psi(2S)\phi$  [13],  $B_s^0 \rightarrow D_s^+ D_s^-$  [14],  $B_s^0 \rightarrow J/\psi K^+ K^-$  where the high  $K^+ K^-$  mass range is considered [15],  $B_s^0 \rightarrow J/\psi K^+ K^-$  [7] and  $B_s^0 \rightarrow J/\psi\pi^+\pi^-$  [8]. An updated combination has been performed, including the two new  $B_s^0 \rightarrow J/\psi h^+ h^-$  analyses presented here. The results are displayed in Fig. 6.

The combined results for the  $b \rightarrow c\bar{c}s$  parameters are outlined in Tab. IV. The experimental precision of the measurements presented has improved tremendously with the inclusion of the new measurements.

## VII. CONCLUSION

LHCb is currently producing some of the world's most precise measurements in terms of CP-violation

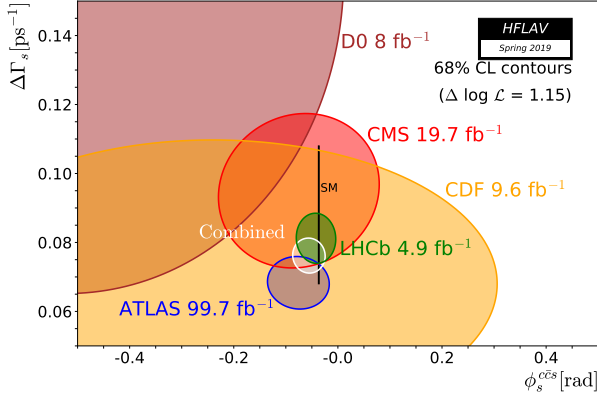


FIG. 6: Updated experimental status of  $\phi_s^{c\bar{c}s}$  vs.  $\Delta\Gamma_s$  with the inclusion of the Run 2  $B_s^0 \rightarrow J/\psi K^+ K^-$  and  $B_s^0 \rightarrow J/\psi \pi^+ \pi^-$  results.

TABLE IV: Updated  $b \rightarrow c\bar{c}s$  combination results

Parameter	Fit Result
$\phi_s^{c\bar{c}s}$	$-0.041 \pm 0.025$ [rad]
$ \lambda $	$0.993 \pm 0.010$
$\Gamma_s$	$0.6562 \pm 0.0021$ [ps $^{-1}$ ]
$\Delta\Gamma_s$	$0.0816 \pm 0.0048$ [ps $^{-1}$ ]

in  $B_s^0$  meson decays. The results presented do not

yet include the data taken at LHCb in 2017 and 2018 and it will be very interesting to further increase the precision by including more data. The expected in-

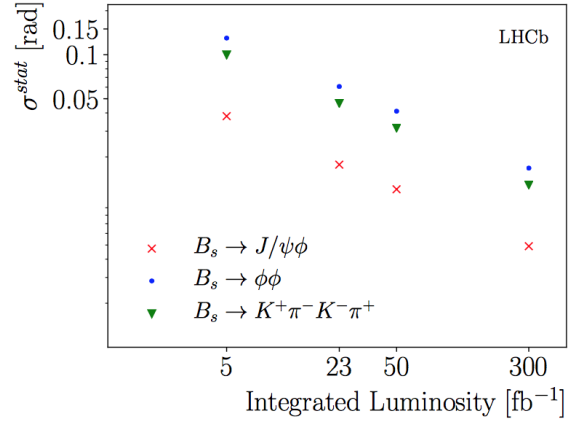


FIG. 7: Comparison of  $\phi_s$  statistical sensitivity from different decay modes.

crease in sensitivity of  $B_s^0 \rightarrow \phi\phi$ ,  $B_s^0 \rightarrow J/\psi K^+ K^-$  and  $B_s^0 \rightarrow K^+ \pi^- K^- \pi^+$  is shown in Fig. 7, where the current results are based on a sample of data corresponding to  $5\text{fb}^{-1}$ .

- 
- [1] R. Aaij et al. (LHCb collaboration) (2019), in preparation.
- [2] H.-Y. Cheng and C.-K. Chua, Phys. Rev. D **80**, 114026 (2009), URL <https://link.aps.org/doi/10.1103/PhysRevD.80.114026>.
- [3] M. Bartsch, G. Buchalla, and C. Kraus (2008), 0810.0249.
- [4] T. Moroi, Physics Letters B **493**, 366 (2000), ISSN 0370-2693, URL <http://www.sciencedirect.com/science/article/pii/S0370269300011606>.
- [5] S. Nandi and A. Kundu, Journal of Physics G: Nuclear and Particle Physics **32** (2006).
- [6] Physics Letters B **671**, 256 (2009), ISSN 0370-2693, URL <http://www.sciencedirect.com/science/article/pii/S0370269308014731>.
- [7] R. Aaij et al. (LHCb collaboration), Phys. Rev. Lett. **114**, 041801 (2015), 1411.3104.
- [8] R. Aaij et al. (LHCb collaboration), Phys. Lett. **B736**, 186 (2014), 1405.4140.
- [9] R. Aaij et al. (LHCb collaboration) (2019), in preparation.
- [10] Y. Amhis et al. (Heavy Flavour Averaging Group), Eur. Phys. J. **C77**, 895 (2017), 1612.07233.
- [11] R. Aaij et al. (LHCb collaboration), Phys. Rev. **D89**, 092006 (2014), 1402.6248.
- [12] *Ckmfitter global fit results as of summer 18*, [http://ckmfitter.in2p3.fr/www/results/plots\\_summer18/num/ckmEval\\_results\\_summer18.html](http://ckmfitter.in2p3.fr/www/results/plots_summer18/num/ckmEval_results_summer18.html), accessed: 2019-05-21.
- [13] R. Aaij et al. (LHCb collaboration), Phys. Lett. **B762**, 253 (2016), 1608.04855.
- [14] R. Aaij et al. (LHCb collaboration), Phys. Rev. Lett. **113**, 211801 (2014), 1409.4619.
- [15] R. Aaij et al. (LHCb collaboration), JHEP **08**, 037 (2017), 1704.08217.